Characteristics of Solution-Processed Small-Molecule Organic Films and Light-Emitting Diodes Compared with their Vacuum-Deposited Counterparts

By *Tae-Woo Lee,* Taeyong Noh, Hee-Won Shin, Ohyun Kwon, Jong-Jin Park,* Byoung-Ki Choi, Myeong-Suk Kim, Dong Woo Shin,* and *Yong-Rok Kim*

Although significant progress has been made in the development of vacuum-deposited small-molecule organic light-emitting diodes (OLEDs), one of the most desired research goals is still to produce flexible displays by low-cost solution processing. The development of solution-processed OLEDs based on small molecules could potentially be a good approach but no intensive studies on this topic have been conducted so far. To fabricate high-performance devices based on solution-processed small molecules, the underlying nature of the produced films and devices must be elucidated. Here, the distinctive characteristics of solution-processed small-molecule films and devices compared to their vacuum-deposited counterparts are reported. Solution-processed blue OLEDs show a very high luminous efficiency (of about 8.9 cd A^{-1}) despite their simplified structure. A better hole-blocking and electron-transporting layer is essential for achieving high-efficiency solution-processed devices because the solution-processed emitting layer gives the devices a better hole-transporting capability and more electron traps than the vacuum-deposited layer. It is found that the lower density of the solution-processed films (compared to the vacuum-deposited films) can be a major cause for the short lifetimes observed for the corresponding devices.

1. Introduction

The standard method for fabricating organic light-emitting diodes (OLEDs) based on small molecules is vapor deposition of the materials through a series of physical shadow masks.[1,2] However, this process has critical drawbacks including considerable loss of the expensive materials during evaporation, and high manufacturing costs. The best way to improve the efficiency of the process and reduce the production costs is to use solution processing of the OLED materials. Ink-jet printing, for example, can be effectively used to fabricate large-area, high-resolution, fast-response, and full-color flat or flexible panel displays. Currently, it is particularly difficult to obtain high-performance flexible panel devices by using other displays, such as liquid-crystal or electrophoretic ones. Although significant progress has been made to obtain highly efficient and stable vacuum-deposited small-molecule OLEDs, reports on the fabrication of such devices by means of solution processing are relatively scarce.[3,4] Therefore, we have focused on the development of solution-processed small-molecule OLEDs to avoid the high manufacturing costs related to vacuum deposition. Although light-emitting polymers are considered to be a suitable form for solution printing, their performance must be further improved for applications in commercial active-matrix OLED devices.[5,6] The efficiency and lifetime of vacuum-deposited small-molecule OLEDs significantly outperform those of the polymer-based devices.[6,7] Therefore, it would be a good strategy to develop OLED devices based on soluble small molecules; this would be a significant step toward the commercialization of ink-jet-based OLEDs for flat or flexible panel full-color displays. In this respect, it is necessary to investigate the distinctive nature of the films and devices fabricated using solution-processed small molecules compared to

[*] Dr. T.-W. Lee, Dr. J.-J. Park, Dr. T. Noh, Dr. O. Kwon, Dr. B.-K. Choi, Dr. M.-S. Kim, Dr. D. W. Shin
Display Device and Processing Laboratory
Samsung Advanced Institute of Technology
Mt. 14-1, Nongseo-dong, Giheung-gu, Yongin-si
Gyeonggi-do 446-712 (Korea)
E-mail: twlee@postech.ac.kr; jongjin00.park@samsung.com

Dr. T.-W. Lee
Department of Materials Science and Engineering
Pohang University of Science and Technology
San 31 Hyoja-dong, Nam-gu, Pohang
Gyeongbuk 790-784 (Korea)

Dr. H.-W. Shin, Prof. Y.-R. Kim
Photon Applied Functional Molecule Research Laboratory
Department of Chemistry
Yonsei University
Seoul 120-749 (Korea)

DOI: 10.1002/adfm.200801045

those obtained by vacuum deposition. Since most of the small molecules designed for vacuum deposition are not suitable for solution processing, we chose 2-(*t*-butyl)-9,10-bis(2′-naphthyl) anthracene (TBADN) as the emitting host material – a compound that can be used both in solution-processing and vacuum-deposition methods.

We fabricated blue-emitting small-molecule OLEDs by solution processing using TBADN (doped with 4,4′-bis[2-{4-(*N*,*N*-diphenylamino)phenyl}vinyl], DPAVBi) as the emitting material because of its good solubility and film-forming properties. We investigated the morphological and photophysical properties of the solution-processed films by atomic force microscopy (AFM), picosecond time-resolved photoluminescence (PL) spectroscopy, and spectroscopic ellipsometry. We also studied the electrical and electro-optical properties of solution-processed hole-only and bipolar devices – regarding hole-transport capability and charge trapping – as well as their current–voltage–luminance (*I*–*V*–*L*) characteristics. The obtained results are compared herein with the characteristics of vacuum-deposited films and devices (in terms of luminous efficiency and operational lifetime).

2. Results and Discussion

To investigate the distinctive nature of solution-processed small-molecule films, the quality of such films must be similar to that of their vacuum-deposited counterparts. First, we compared the morphology of the solution-processed films with that of vacuum-deposited films. To do this, we dissolved the DPAVBi-doped TBADN (95w/5w) in toluene and chlorobenzene. After spin-coating, the films were baked for 15 min (at 100 °C) on a hot plate under N_2 atmosphere. Figure 1 shows the AFM images of both types of film. The root-mean-square (RMS) roughness values of spin-cast films obtained from toluene and chlorobenzene solutions were 0.655 and 0.520 nm, respectively. These values are quite similar to that of a vacuum-deposited film (i.e., 0.575 nm). It must be noted, however, that the film obtained from the toluene solution exhibited a kind of aggregation, or phase segregation, which was not observed in the layer obtained using the chlorobenzene solution.

We then fabricated OLED devices using the solution-processed films as the emitting layer (EML) and aluminum tris(8-hydroxyquinoline) (Alq_3) or 1,3,5-tris(2-*N*-phenylbenzimidazolyl) benzene (TPBI) as electron-transporting layers. Figure 2 shows the *I*–*V*–*L* characteristics of the devices. We first compared the solution-processed device with the corresponding vacuum-processed device using Alq_3 as the electron-transporting layer in both cases. Figure 2a and b shows that the current density and the luminance of the solution-processed device are much higher, at fixed voltages, than those of a vacuum-deposited device with the same structure. Although the operating voltages were lower in the solution-processed devices, the turn-on voltage remained the same (about 2.8 V). Therefore, the improved current and luminance can be attributed to the increased charge-carrier mobilities of the spin-cast films rather than to lower charge-injection barriers in the solution-processed devices.

We observed the transient electroluminescence (EL) of solution-processed OLEDs by using a 10 V voltage pulse and 1 Hz frequency (see Fig. 3). We defined the saturation time (t_s) of luminescence after switching-on as 90% of the maximum light

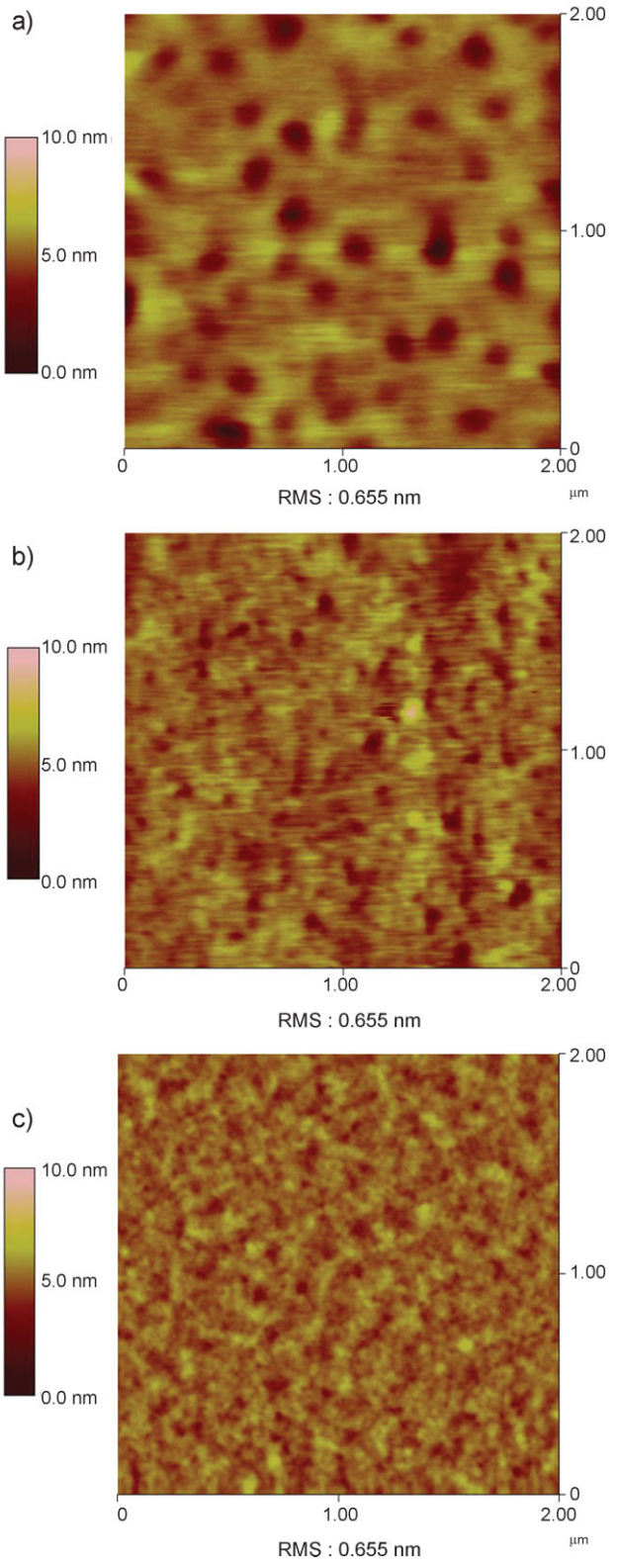

Figure 1. AFM images of spin-cast TBADN/DPAVBi films (95w/5w) obtained from a) toluene, b) chlorobenzene solutions, and c) a vacuum-deposited film.

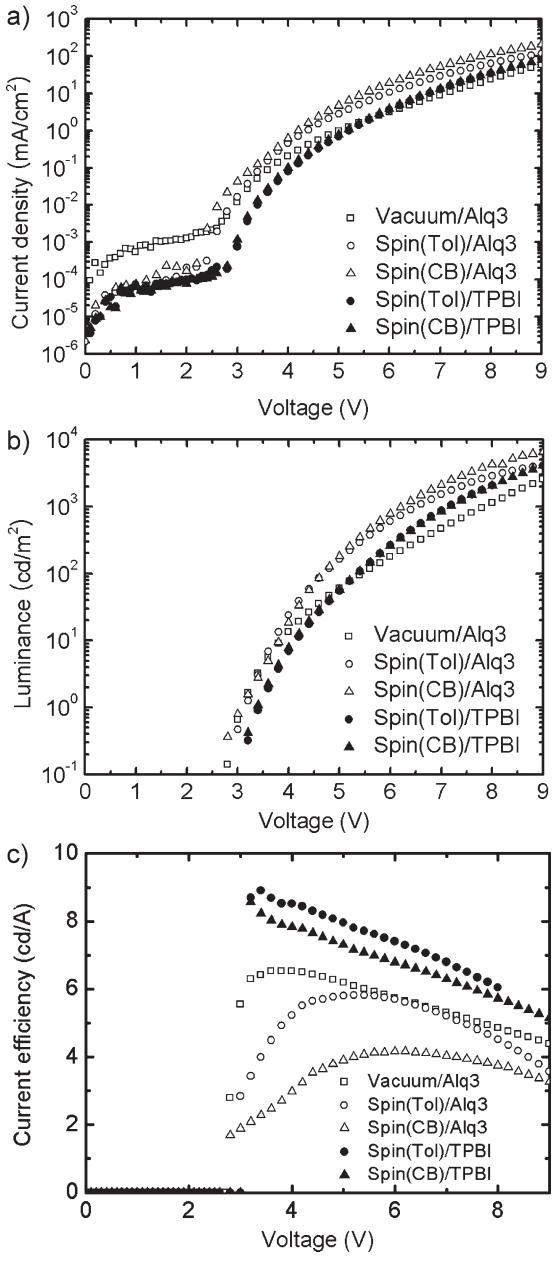

Figure 2. Characteristics of solution-processed and vacuum-deposited bipolar (a–c) and hole-only devices (d) of ITO/PEDOT:PSS/TBADN+D-DPAVBi/Alq_3/LiF/Al and ITO/PEDOT:PSS/TBADN (130 nm)/Au structures, respectively. a) Current density versus voltage of bipolar devices, b) luminance versus voltage of bipolar devices, and c) current efficiency versus voltage of bipolar devices.

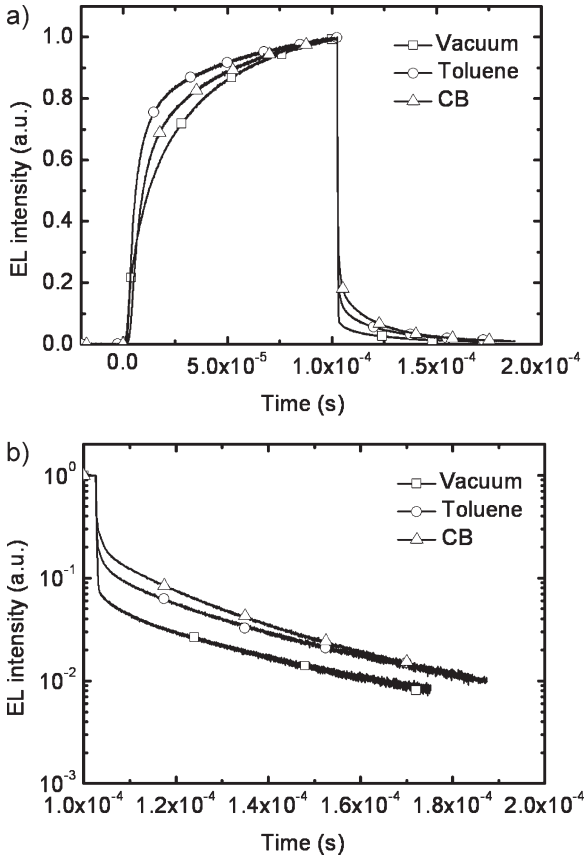

Figure 3. Transient electroluminescence characteristics of solution-processed (toluene and chlorobenzene, CB) and vacuum-deposited devices of ITO/PEDOT:PSS/TBADN+DPAVBi /Alq_3/LiF/Al structure. A linear plot versus time (a) to show the rising characteristics of the transient electroluminescence and a semilogarithmic plot versus time (b) to investigate the decay of the transient electroluminescence. A low-duty-cycle electrical pulse (100 μs pulse width, 10 Hz pulse frequency) produced by a pulse/function generator was applied to the device.

intensity. The t_s value of the devices strongly depends on the film-forming process of the EML, whereas the delay time (i.e., the time difference between voltage onset and the appearance of an EL signal) only changes slightly. The HOMO levels of TBADN and Alq_3 are almost the same (about −5.8 eV) so that there is apparently no hole-blocking barrier between the EML and the Alq_3 layer.[8] Since the dopant (DPAVBi) does not act as a trap in the matrix,[9] we consider that the charge-transport mobilities of the matrix should be very similar to those of TBADN. The electron mobility of Alq_3 ($\approx 3 \times 10^{-7}\,cm^2\,V^{-1}\,s^{-1}$ at $0.8\,MV\,cm^{-1}$) is similar to the hole mobility of TBADN ($\approx 2 \times 10^{-7}\,cm^2\,V^{-1}\,s^{-1}$ at $0.6\,MV\,cm^{-1}$), which is at the same time two orders of magnitude greater than the hole mobility of Alq_3 ($\approx 2 \times 10^{-9}\,cm^2\,V^{-1}\,s^{-1}$ at $0.8\,MV\,cm^{-1}$). The reason for this behavior is that TBADN shows ambipolar transport characteristics.[10] This contrast in the mobilities can make holes accumulate at the EML/Alq_3 interface so that electron–hole recombination will take place as soon as the electrons arrive at the interface. As a result, the t_s values can be related to the traveling distance of the electrons within the devices before they recombine with the holes. The t_s of a solution-processed device obtained from a toluene solution is faster (i.e., 41.64 μs) than that of a device produced from a chlorobenzene solution (52.3 μs), and this is in turn faster than that of a vacuum-processed device (59.7 μs). The device fabricated using a spin-cast film obtained from the toluene solution also shows the shortest EL rising time (whereas the vacuum-processed film exhibits the longest EL rising time).

If the hole transport mobility of the EML becomes faster by solution-processing, the recombination zone should be located closer to the EML/Alq_3 interface as depicted in Figure 5. In this case, the traveling distance of the electrons before recombination may become shorter, causing the t_s value to decrease. From this viewpoint, the transient EL behavior can be explained by a difference in the hole transport mobility of the EML. Figure 3b shows the luminance-decay behaviors observed after turning-off the devices. The decay time of the solution-processed devices is obviously slower than that of the vacuum-processed devices, which implies that the former devices possess more charge traps. Since we observed increased current densities in the case of the solution-processed devices (compared to the vacuum-processed ones, see Fig. 4), we concluded that electron traps – rather than hole traps—are induced. In this case, electron transport within the EML can be reduced so that electron–hole recombination will mostly take place near the electron-transporting layer. Thus, solution processing may lead to a reduction in the electron transport mobility as a result of electron charge traps.

A previous study reported that one characteristic feature of organic semiconductors is strong trapping of electrons, which resulted in very low electron mobility in transistors.[11] If we consider the origin of the electron traps in the solution-processed films, we find that soluble small molecules can exclude catalysts – unlike solution-processed polymer films. Since the molecules in the films obtained by solution processing are not as closely packed as those in the vacuum-based layers (a result that is supported by ellipsometry data presented below, see Fig. 8), solvent impurities may remain inside the solution-processed films much easier and oxygen can diffuse into the film more easily. The solvent impurities and diffused oxygen could be a plausible cause for the formation of electron traps. In the solution-processed devices, the recombination zone is located closer to the Alq_3 layer because of the reduced electron mobility and increased hole mobility of the EML; this characteristic should cause the luminous efficiency of solution-processed devices to be lower than that of vacuum-processed devices. The similar HOMO levels at the interface between EML and Alq_3 make hole blocking much more ineffective (see Fig. 5), especially in the case of solution-processed devices, which have increased hole mobilities and exhibit electron traps in the EML. Therefore, the luminous efficiency of solution-processed devices fabricated using an Alq_3 layer was lower (see Fig. 2c).

We solved the problem of low luminous efficiency of the solution-processed devices by using TPBI (instead of Alq_3) as the electron-transporting layer (see Fig. 5). As shown in Figure 2c, the luminous efficiency of the devices could be greatly improved – up to 8.9 cd A^{-1}, which is a very high value in this simplified device structure prepared without using a hole-transporting layer on top of the poly(3,4-ethylenedioxythiophene):poly(styrene sulfonate) (PEDOT:PSS) layer. Figure 4 shows the *I–V* characteristics of hole-only devices fabricated with an Au contact. The device prepared from the toluene solution showed the largest current densities, whereas the vacuum-deposited device showed the lowest current densities. This can be attributed to the different morphological characteristics of the films, which depend on the film-forming processes. The local molecule aggregation observed in the films cast from the toluene solution (see Fig. 1) provides an efficient charge-transport pathway, which results in an increased current density. On the other hand, the devices prepared using the chlorobenzene solution showed lower current densities because of their significantly reduced molecular aggregation. The vacuum-deposited films are quite amorphous; hence the current densities of devices based on such films may be lower than those of other films composed of aggregated films.

Time-resolved PL measurements showed that the solution-processed films (toluene) had slightly shorter PL lifetimes (namely, $\tau_1 = 150$ ps and $\tau_2 = 800$ ps) than the vacuum-deposited ones (i.e., $\tau_1 = 185$ ps and $\tau_2 = 865$ ps, see Fig. 6). This finding can be attributed to an excitation-energy transfer to the local aggregates occurring as a result of the smaller bandgap generated by the stronger intermolecular π–π interactions. The very slight changes observed in the PL lifetimes of solution-processed films imply that no critical luminescent-quenching centers were induced during film formation, which is the reason why we

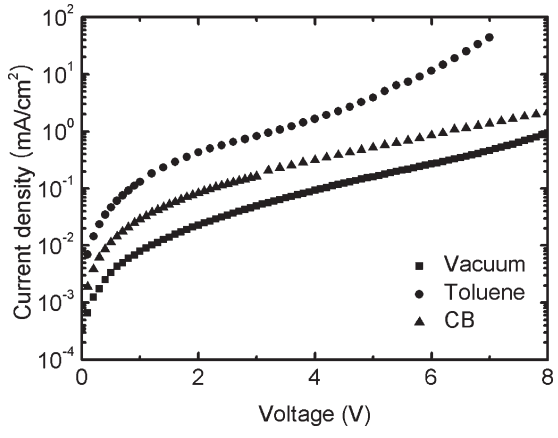

Figure 4. Current density versus voltage characteristics of solution-processed (toluene and chlorobenzene, CB) and vacuum-deposited hole-only devices of ITO/PEDOT:PSS/TBADN (130 nm)/Au structure.

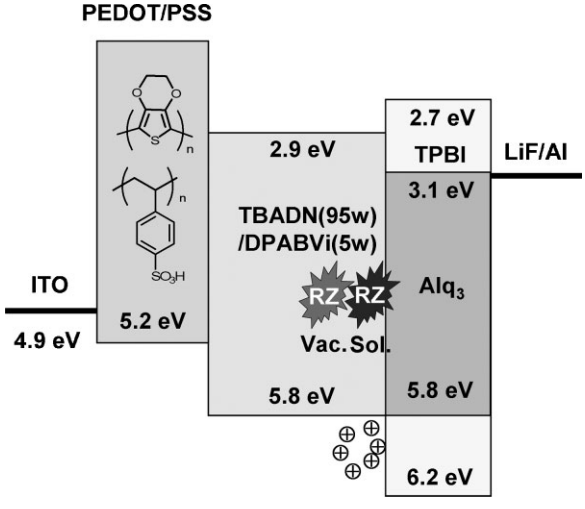

Figure 5. The schematic energy diagram of ITO/PEDOT:PSS/TBADN+D-DPAVBi /Alq_3/LiF/Al and ITO/PEDOT:PSS/TBADN+DPAVBi/TPBI/LiF/Al devices. We compared the recombination zone (RZ) of the solution-processed devices with the vacuum-deposited counterparts.

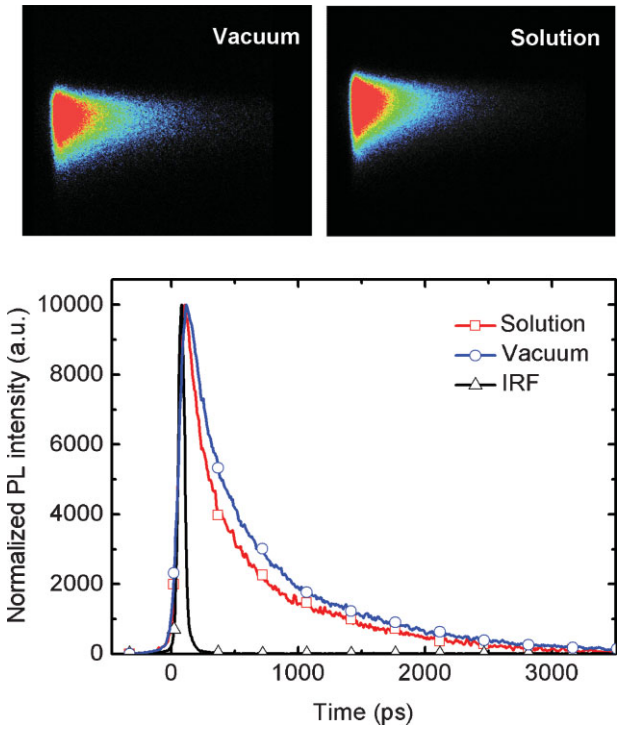

Figure 6. Transient photoluminescence characteristics of the solution-processed (toluene) and vacuum-deposited films. IRF denotes instrument response function. The upper panels show streak camera images.

achieved highly efficient solution-processed devices and raises hope for further improvement.

We also studied the lifetimes of the devices (see Fig. 7) and found that they were significantly shorter for the solution-processed devices than for the vacuum-processed ones. The devices processed from the chlorobenzene solution exhibited longer lifetimes than those obtained from the toluene solution, although the efficiency was lower. The device lifetime was strongly dependent on the film-

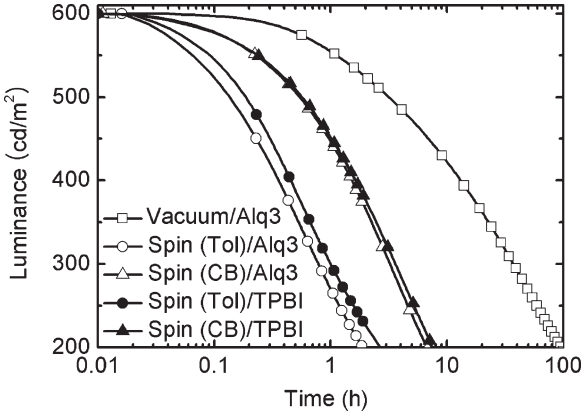

Figure 7. Luminance decay versus time characteristics of solution-processed (toluene and chlorobenzene, CB) of ITO/PEDOT:PSS/TBADN+D-DPAVBi/Alq_3(or TPBI)/LiF/Al structure and vacuum-deposited devices of ITO/PEDOT:PSS/TBADN+DPAVBi/Alq_3/LiF/Al structure under an electrical current stress (at an initial brightness of 600 cd m^{-2}).

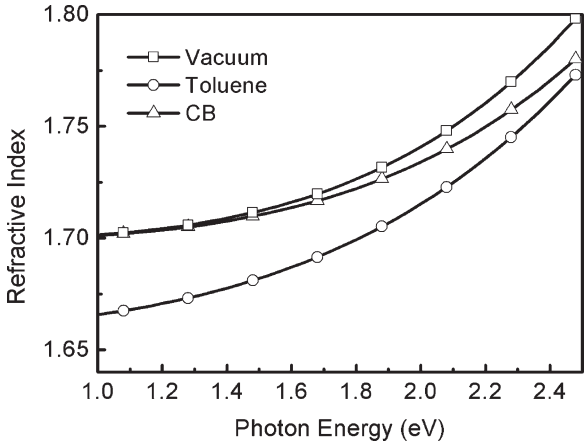

Figure 8. Spectroscopic ellipsometry data of solution-processed (toluene and chlorobenzene, CB) and vacuum-deposited TBADN films.

processing conditions, regardless of the kind of electron-transporting layer used (Alq_3 or TPBI). This result indicates that the crucial factor determining the device lifetime is film morphology. We sought to investigate the intrinsic characteristics of the spin-processed films by performing spectroscopic ellipsometry measurements on a silicon wafer covered with native oxide (2.07 nm) (VB-250 VASE ellipsometer, J. A. Woolam Co. Inc). Figure 8 shows the ordinary refractive index versus the photon energy for the three types of films. These ellipsometry measurements provide information about the film density. The ordinary refractive index of the spin-cast film obtained from the toluene solution is much lower than that of the vacuum-deposited film, which can be attributed to the presence of free volume inside the former layer. The film obtained from the chlorobenzene solution, however, has a refractive index that is only slightly below that of the vacuum-deposited film. The ellipsometry data are in good agreement with the AFM data. If we correlate these ellipsometry data with the device lifetimes, we can conclude that the major cause of the reduction in the lifetime of solution-processed devices is the lower film density, which is caused by the presence of free volume between the aggregates inside the film. Therefore, we suggest that the lifetime of solution-processed devices could be improved by controlling the film morphology so as to increase the density of the obtained layers.

3. Conclusions

The OLEDs fabricated using solution-processed films showed very high device efficiencies (up to about 8.9 cd A^{-1}). Because solution processing causes local aggregation within the films, hole transport is significantly enhanced in the solution-processed devices compared to the vacuum-processed ones. On the other hand, more electron traps are generated in the solution-processed devices, thus limiting electron transport through the EMLs. Therefore, electron–hole recombination takes place close to the electron-transporting layer, which means that a film with good hole-blocking characteristics is required. Solution-processed films are less dense than their vacuum-deposited counterparts, which can be a major cause for the short lifetime of

solution-processed devices. To improve the device lifetime, research should focus on the film density. To the best of our knowledge, this work is the first study showing the characteristics of solution-processed small-molecule organic films and devices compared to those of their vacuum-deposited analogues. Therefore, our results can be used as a guide to improve the performance of organic electronic or optoelectronic devices based on solution process of small molecules, including organic memories, organic thin-film transistors, organic photovoltaic cells, and OLEDs.

4. Experimental

4.1. OLED Fabrication and Characterization

DPAVBi-doped TBADN (95w/5w) (LumTec Corp.) was dissolved in toluene and chlorobenzene. A water-dispersed PEDOT/PSS mixture (Baytron P VP AI4083, H. C. Starck GmbH) was spin-coated on top of UV/ozone treated indium tin oxide (ITO) in air to achieve films with a thickness of 50 nm. The spin-coated films were baked on a hot plate at 110 °C for 5 minutes in air and 200 °C for 5 minutes in an N_2 glove box. The emitting layer was deposited either by spin-coating or by vacuum evaporation (at a pressure below 3×10^{-7} Torr) to obtain a thickness of 80 nm. The solution-processed films were baked on a hot plate (110 °C, 5 min) in an N_2 glove box. Electron-transporting layers (Alq_3 or TPBI, LumTec Corp.) with a thickness of 20 nm were deposited by vacuum evaporation. LiF (1 nm) and Al (150 nm) films were sequentially deposited on the electron-transporting layer under vacuum (below 5×10^{-7} Torr). The OLED devices were encapsulated with a glass lid using an epoxy resin. Their *I–V–L* characteristics were obtained using a Keithley 238 source-measure unit and a Photo Research PR650 spectrophotometer. The capacitance–voltage measurements were performed using an impedance analyzer (Solartron 1260).

4.2. Transient Electroluminescence Measurements

For the transient EL measurements, a low-duty-cycle electrical pulse (100 μs pulse width, 10 Hz pulse frequency) produced by an HP 8116A 50 MHz pulse/function generator was applied to the device. The low duty cycle of the electrical pulses can minimize any device heating and reduces the number of residual space charges present after each switch-off of the voltage pulse. The emitted light was detected by using a photomultiplier tube assembly (HC125-01, Hamamatsu Corp.; Rise-time: 1.5 ns). The pulse shape and the photodetector output signal were measured by an oscilloscope (Agilent Infinium 54830B oscilloscope 600 MHz 4GSa/s).

4.3. Picosecond Time-Resolved PL Spectroscopy Using a Streak Camera

For the time-resolved PL studies, all the samples were excited using picosecond pulses ($\lambda = 315$ nm) generated by a Raman shifter (18 atm, CH_4), which was pumped by the fourth-harmonic pulse (266 nm, FWHM 20 ps, 10 Hz) of a mode-locked Nd:YAG laser (Continuum, Leopard D10). Time-resolved PL spectra and decay data were detected with a picosecond streak camera (Optronis, SCMU-ST-S20) coupled to a spectrometer (CVI, DKSP240) and a charge-coupled device (CCD) system (Optronis, SCRU-SE-S). The typical accumulation number for a PL spectrum was 400 laser shots. Fitting of the PL decays was carried out by using a nonlinear least-squares iterative-deconvolution method.

4.4. Variable-Angle Spectroscopic Ellipsometry

Spectroscopic ellipsometry measurements were performed at incidence angles of 65, 70, and 75° using a variable-angle ellipsometer (VB-250 VASE ellipsometer, J. A. Woolam Co. Inc) with an autoretarder in the spectral range of 1.0–4.5 eV. The possibility of using multiple angles of incidence increases the accuracy in determining the dielectric function of the layer from pseudodielectric functions, which were fitted using the nonlinear Levenberg–Marquardt algorithm (with the WVASE32 software), assuming an organic layer on a silicon substrate. In order to estimate the dielectric functions of the organic layers, we adopted the well-known Cauchy model.

Acknowledgements

Y.-R. K. acknowledges a grant from the Korea Science and Engineering Foundation (KOSEF) (Grant No. R0A-2003-000-10305-0). The paper submission has been approved by the internal committee in Samsung Advanced Institute of Technology on August 22, 2007. The approval tracking code number is 20070822090824700E. This article appears as part of a special issue on materials science in Korea.

Received: July 23, 2008
Revised: February 4, 2009
Published online: March 30, 2009

[1] C. W. Tang, S. A. VanSlyke, *Appl. Phys. Lett.* **1987**, *51*, 913.
[2] M. A. Baldo, D. F. O'Brien, Y. You, A. Shoustikov, S. Sibley, M. E. Thompson, S. R. Forrest, *Nature* **1998**, *395*, 151.
[3] M. O'Regan, D. Lecloux, C. Hsu, E. Smith, A. Goenaga, C. Lang, in the proceedings of the *IMID/IDMC'06 Digest*, Korea **2006**, p. 1689.
[4] a) S. Kato, *J. Am. Chem. Soc.* **2005**, *127*, 11538. b) Y. Hino, H. Kajii, Y. Ohmori, *Org. Electron.* **2004**, *5*, 265.
[5] J. H. Burroughes, presented at the Asia Display/IMID'2004, Daegu, Korea, August **2004**.
[6] H. K. Chung, presented at the IMID'2005, Seoul, Korea, July **2005**.
[7] M. S. Weaver, Y.-J. Tung, B. D'Andrade, J. Esler, J. J. Brown, C. Lin, P. B. Mackenzie, R. W. Walters, J.-Y. Tsai, C. S. Brown, S. R. Forrest, M. E. Thompson, *Soc. Information Display Digest Tech. Pap.* **2006**, *37*, 127.
[8] S. C. Tse, S. K. So, M. Y. Yeung, C. F. Lo, S. W. Wen, C. H. Chen, *Jpn. J. Appl. Phys.* **2006**, *45*, 555.
[9] Y.-C. Tsai, J.-H. Jou, *Appl. Phys. Lett.* **2006**, *89*, 243521.
[10] J.-H. Lee, Y.-H. Ho, T.-C. Lin, C.-F. Wu, *J. Electrochem. Soc.* **2007**, *154*, J226.
[11] L.-L. Chua, J. Zaumseil, J.-F. Chang, E. C.-W. Ou, P. K.-H. Ho, H. Sirringhaus, R. H. Friend, *Nature* **2005**, *434*, 194.